

RESEARCH ARTICLE

Road Roughness Identification in Vehicle Dynamics: The Role of Measurements in Ensuring System Observability

ANTONIO LEANZA¹, SIMONE DE CAROLIS¹, LEONARDO SORIA¹,
AND GIUSEPPE CARBONE^{1,2}

¹Department of Mechanics, Mathematics and Management, Politecnico di Bari, 70125 Bari, Italy

²Physics Department M. Merlin, CNR Institute for Photonics and Nanotechnologies U.O.S. Bari, 70126 Bari, Italy

Corresponding author: Antonio Leanza (antonio.leanza@poliba.it)

This work was supported in part by the Italian Ministry of Education, University and Research (Program Department of Excellence: Legge 232/2016).

ABSTRACT Dynamical systems, as, specifically, vehicles' models, often rely on unknown inputs and on states that may not be directly measured. This represents a challenging research topic, for which various methods and solutions have been proposed. The present study focuses on the recovery of road roughness and the estimation of vertical dynamics states using a quarter-car model and two Kalman filtering-based approaches, even comparing their performance in terms of accuracy, robustness, and computational efficiency. The application of these algorithms may face issues due to certain measurements that are not readily available, impacting system observability. This aspect is thoroughly investigated by collecting different methods scattered in the scientific literature and introducing a new parameter derived from the entries of the observability matrix. Through numerical simulations and a carefully designed experiment, in this effort, we identify critical measurements and determine the most effective method for estimating quantities that are not directly measurable.


INDEX TERMS Kalman filter, unknown inputs, road identification, vehicle dynamics, system observability.

I. INTRODUCTION

In almost all real-world engineering applications, several system quantities do exist, that may be not directly measurable for practical or economic reasons [1], [2]. Nonetheless, the knowledge of their values over time is crucial for control purposes and to guarantee the correct system operation and safety [3]. Among these unknown variables, we may find both states and inputs acting on the system [4], [5], [6]. A large number of methods have been, in fact, developed over the years, to treat this topic, such as those reported in Refs. [7], [8], [9], and [10] and many others. In vehicle dynamics, these circumstances are encountered in the study of suspension behaviour, when no information regarding the road surface roughness is available. The problem of unknown states' estimation and road input recovery has been faced by exploiting different techniques in the literature [4], [11], [12],

[13], [14], [15], which are grounded on Kalman filtering-based approaches.

Different types of Kalman Filter (KF)-based observers have been developed for estimating states in the case of systems with unknown inputs. To offer examples, in [16] a Two-stage KF unaffected by the unknown inputs is proposed, whilst in [17] a Three-stage KF is introduced to estimate fault and state together with unknown inputs. The majority of the existing methods have been conceived for systems not affected by unknown exogenous inputs or *vice versa*, assuming that the unknown inputs matrix has full column rank. To overcome this limitation, in Ref. [18] a recursive filter approach has been proposed, referred to as General Kalman Filter with Unknown Inputs (GKF-UI). This estimator has also been exploited in [4] and [12]. Although several algorithms have been developed for the recovery of the unknown inputs during state estimation, one direct solution relies on augmenting the state vector to incorporate the unknown inputs [19], [20], [21]. Whenever a model

The associate editor coordinating the review of this manuscript and approving it for publication was Jjun Cheng .

for the unknown inputs is available, an optimal estimator can be employed. Otherwise, suitable models should be assumed to perform the joint estimation, achieving a sub-optimal solution. In this paper, we, in particular, show the advantages of using an augmented state vector to perform the estimation. These benefits include both the quality of the achieved estimates and the improvement of the computational efficiency.

Regardless of the algorithm selected to perform the estimation of non-measurable quantities, the observability of the considered dynamical system plays a key role. Specifically, observability indicates to what extent system states and unknown inputs may be inferred from the available measurements [22]. By the present research, we discuss both how many and which kind of measurements do affect the observability of the dynamical system in analysis. We specifically study the case of the celebrated Quarter-Car (QC) model, subjected to the usually unknown road input excitation. Through numerical simulations and an experimental setup, the critical measurement is identified, and the quality of the system observability is investigated, by considering different sets of measurements. We show that the dynamical system observability strongly depends on a specific measurement not always directly available in the engineering practice. Although the obtained results refer to the dynamical system at hand, the study is relevant for different practical scenarios, highlighting the importance of a correct selection of measurements, regardless of how many they are. In the paper, we moreover highlight that the joint estimation via augmented states allows for a deeper study of the quality of the system observability, against other kinds of KF-based estimators, such as the GKF-UI.

The rest of the paper is organized as follows. Section II introduces the system model and the characteristics of typical road profiles and briefly describes two Kalman filtering-based approaches for the estimation of non-measurable states with input reconstruction for Linear Time-Invariant (LTI) dynamical systems. The problem of the observability for LTI systems with unknown inputs is thoroughly investigated in Section III. Section IV deals with the practical problem discussed before, translated in the automotive field through a LTI dynamical system with unknown input in a numerical fashion, and in Section V we develop an experimental setup for the same system and discuss the obtained results. Finally, in Section VI conclusions are drawn.

II. SYSTEM FOR ROAD PROFILES IDENTIFICATION

Roads are random surfaces [23]. In the frequency domain, a typical road surface spectrum is characterized by higher energy at long wavelengths and gradually less energy at increasingly shorter wavelengths [24]. This behaviour also holds for every profile associated with a generic road, as depicted in Figure 1 (a).

Road profiles produce the so-called road input excitation on vehicle systems, primarily described by the well-known Quarter-Car (QC) model, shown in Figure 1 (b) and

extensively used in automotive engineering to investigate vehicle vertical vibrations. It represents an example of a Linear Time-Invariant (LTI) dynamical system, with unknown inputs for the case of road identification, along with the unknown states estimation, such as, e.g., the sprung mass displacement. A generic LTI system with unknown inputs unfolds the following set of process and measurement equations

$$\begin{cases} \dot{\mathbf{x}} = \mathbf{A}\mathbf{x} + \mathbf{B}\mathbf{u} + \mathbf{B}^*\mathbf{u}^* \\ \mathbf{y} = \mathbf{C}\mathbf{x} + \mathbf{D}\mathbf{u} + \mathbf{D}^*\mathbf{u}^* \end{cases} \quad (1)$$

where $\mathbf{x} \in \mathbb{R}^{n \times 1}$ is the vector of n state variables, $\mathbf{u} \in \mathbb{R}^{p_1 \times 1}$ and $\mathbf{u}^* \in \mathbb{R}^{p_2 \times 1}$ the vector of known and unknown inputs respectively, $\mathbf{y} \in \mathbb{R}^{m \times 1}$ the vector of m measurements, $\mathbf{A} \in \mathbb{R}^{n \times n}$ the state evolution matrix, $\mathbf{B} \in \mathbb{R}^{n \times p_1}$ and $\mathbf{B}^* \in \mathbb{R}^{n \times p_2}$ the known and unknown input matrix respectively, $\mathbf{C} \in \mathbb{R}^{m \times n}$, $\mathbf{D} \in \mathbb{R}^{m \times p_1}$, $\mathbf{D}^* \in \mathbb{R}^{m \times p_2}$ the matrices associated to the m measurements equations. As anticipated, in order to estimate states and unknown inputs for such systems, several algorithms have been implemented over the years. In what follows, two Kalman Filter-based estimators are investigated: the General Kalman Filter with Unknown Input (GKF-UI) introduced in [18] and used for this purpose in [4] and [12], and the Augmented Kalman Filter with Unknown Input (AKF-UI), used in [13] and [14], where the vector of state variables is augmented with unknown inputs. Before dealing with those estimators, the process and measurement uncertainties must be considered in the set of Equations (1). In this research, they are modelled as additive, zero-mean, white, and Gaussian noises. Moreover, both the process and the measurement noises are hypothesized uncorrelated and internally orthogonal. All these assumptions hold for the rest of the paper.

By referring to Figure 1 (b), the following state vector and unknown input is defined

$$\mathbf{x} = [y_1 \quad y_2 \quad \dot{y}_1 \quad \dot{y}_2]^T, \quad \mathbf{u}^* = [h] \quad (2)$$

where the road profile excitation $h(t)$ is the sole input acting on the system, with t the time variable. This leads to the following matrices

$$\mathbf{A} = \begin{bmatrix} 0 & 0 & 1 & 0 \\ 0 & 0 & 0 & 1 \\ -\frac{k}{m_s} & \frac{k}{m_s} & -\frac{c}{m_s} & \frac{c}{m_s} \\ \frac{k}{m_u} & -\frac{k+k_t}{m_u} & \frac{c}{m_u} & -\frac{c}{m_u} \end{bmatrix}, \quad \mathbf{B}^* = \begin{bmatrix} 0 \\ 0 \\ 0 \\ \frac{k_t}{m_u} \end{bmatrix} \quad (3)$$

where m_s and m_u represent the sprung and unsprung mass respectively, k and c are the stiffness and damping coefficients of the suspension system, and k_t represents the

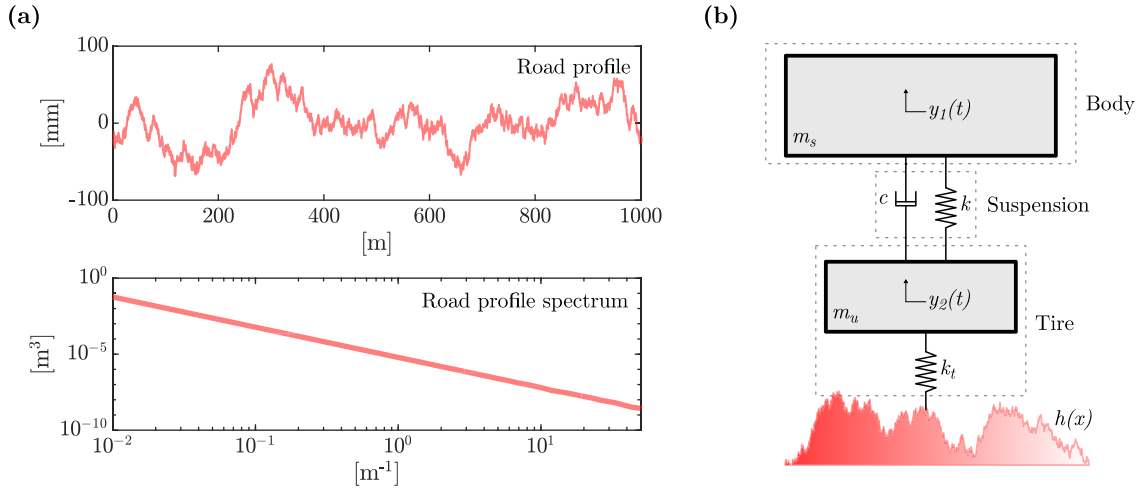


FIGURE 1. A typical road profile representation with its spectrum at the bottom (a) and the quarter-car model (b).

tire stiffness. With regards to the vector \mathbf{y} , of interest is the set of selected measurements

$$\mathbf{y} = [y_1 - y_2 \quad \ddot{y}_1 \quad y_1 \quad \ddot{y}_2]^T \quad (4)$$

where $y_1 - y_2$ represents the suspension travel, \ddot{y}_1 is the sprung mass acceleration, and \ddot{y}_2 the unsprung mass acceleration. These three measurements can be directly obtained by means of commonly adopted sensors, namely two accelerometers and a wheel stroke sensor. Instead, the third component of vector \mathbf{y} is achieved by integrating the sprung mass acceleration \ddot{y}_1 . This measurement is of utmost importance for achieving system observability. Unfortunately, this solution might badly affect actual online applications. Furthermore, if the non-directly measurable states can be got via integration methods, the KF-based estimation becomes actually useless. For this reason, the role played by this particular measurement is thoroughly investigated in Section IV. But already here, we may comment that the drawn conclusions would be similar, if another one of the state variables in \mathbf{x} were included in \mathbf{y} , instead of y_1 , such as e.g. \dot{y}_1 , y_2 , or \dot{y}_2 . It is the effect of adding a so-called canonical row in the measurement matrix \mathbf{C} , namely ensuring the presence of a state directly measured. This last aspect is of general validity for any dynamical system.

A. THE GKF-UI

The GKF-UI introduced in [18] is a recursive algorithm that minimizes an objective function of weighted least squares estimation with respect to the states and unknown inputs. Among the various different-stages KF-based estimators, it comprises very few steps and, thus, it is relatively light in terms of computational effort required. The routine of the GKF-UI is here reported:

Prediction stage

$$\begin{aligned} \hat{\mathbf{x}}_{k|k-1} &= \mathbf{A}\hat{\mathbf{x}}_{k-1|k-1} + \mathbf{B}\mathbf{u}_{k-1} + \mathbf{B}^*\hat{\mathbf{u}}_{k-1}^* \\ \mathbf{P}_{k|k-1} &= \mathbf{A}\mathbf{P}_{k-1|k-1}\mathbf{A}^T + \mathbf{Q} \end{aligned} \quad (5)$$

Kalman gain calculation stage

$$\mathbf{K}_k = \mathbf{P}_{k|k-1}\mathbf{C}^T (\mathbf{C}\mathbf{P}_{k|k-1}\mathbf{C}^T + \mathbf{R})^{-1} \quad (6)$$

Unknown inputs estimation stage

$$\begin{aligned} \mathbf{S}_k &= [\mathbf{D}^*\mathbf{R}^{-1}(\mathbf{I} - \mathbf{C}\mathbf{K}_k)\mathbf{D}^*]^{-1} \\ \hat{\mathbf{u}}_k^* &= \mathbf{S}_k\mathbf{D}^*\mathbf{R}^{-1}(\mathbf{I} - \mathbf{C}\mathbf{K}_k)(\mathbf{y}_k - \mathbf{C}\hat{\mathbf{x}}_{k|k-1} - \mathbf{D}\mathbf{u}_k) \end{aligned} \quad (7)$$

Correction stage

$$\begin{aligned} \hat{\mathbf{x}}_{k|k} &= \hat{\mathbf{x}}_{k|k-1} + \mathbf{K}_k(\mathbf{y}_k - \mathbf{C}\hat{\mathbf{x}}_{k|k-1} - \mathbf{D}\mathbf{u}_k - \mathbf{D}^*\hat{\mathbf{u}}_k^*) \\ \mathbf{P}_{k|k} &= (\mathbf{I} + \mathbf{K}_k\mathbf{D}^*\mathbf{S}_k\mathbf{D}^*\mathbf{R}^{-1}\mathbf{C})(\mathbf{I} - \mathbf{K}_k\mathbf{P}_{k|k-1})\mathbf{P}_{k|k-1} \end{aligned} \quad (8)$$

where $\hat{\mathbf{x}}_{k|k-1}$ is the predicted state vector, $\mathbf{P}_{k|k-1}$ is the predicted error covariance matrix, $\hat{\mathbf{u}}_k^*$ is the estimate of the unknown inputs vector, \mathbf{S}_k is the estimate of the unknown inputs covariance, $\hat{\mathbf{x}}_{k|k}$ is the updated state vector, $\mathbf{P}_{k|k}$ is the updated error covariance matrix, and \mathbf{Q} and \mathbf{R} are the covariance diagonal matrices of process and measurement noise, respectively.

It is worth pointing out that this algorithm has been designed for unknown inputs being present both in the process and the measurement equation. Therefore, the matrices \mathbf{B}^* and \mathbf{D}^* must be different from the null matrix to update the unknown input vector $\hat{\mathbf{u}}_k^*$ in Equation (7) at each time step. Furthermore, the number of the measurements m should be greater than the number of the unknown inputs p_2 to keep the system observable [4], [18].

B. THE AKF-UI

It is possible to perform a reliable joint estimation by augmenting the state vector with the unknown inputs. However, this approach needs an assumption on the model for the evolution of the unknown inputs over time. Whenever no *a priori* information is available about the unknown inputs, a typical model of \mathbf{u}^* is the zero-mean zero-order

random walk driven by a white noise $\mathbf{w}_{\mathbf{u}^*} \sim \mathcal{N}(\mathbf{0}, \mathbf{Q}_{\mathbf{u}^*})$. This procedure is similar to estimating the sensor bias when assuming a constant model over time [25]. Hence, the following state-space system is obtained

$$\begin{cases} \dot{\mathbf{x}} = \mathbf{A}\mathbf{x} + \mathbf{B}\mathbf{u} + \mathbf{B}^*\mathbf{u}^* + \mathbf{G}\mathbf{w} \\ \dot{\mathbf{u}}^* = \mathbf{w}_{\mathbf{u}^*} \\ \mathbf{y} = \mathbf{C}\mathbf{x} + \mathbf{D}\mathbf{u} + \mathbf{D}^*\mathbf{u}^* + \mathbf{v} \end{cases} \quad (9)$$

where $\mathbf{G} \in \mathbb{R}^{n \times n}$ is the matrix associated to the process noise $\mathbf{w} \in \mathbb{R}^{n \times 1}$, and $\mathbf{v} \in \mathbb{R}^{m \times 1}$ is the measurement noise. As said, process and measurement noises are considered white, Gaussian, and orthogonal to each other: $\mathbf{w} \sim \mathcal{N}(\mathbf{0}, \mathbf{Q})$ and $\mathbf{v} \sim \mathcal{N}(\mathbf{0}, \mathbf{R})$. Furthermore, if assumed internally orthogonal, the \mathbf{Q} and \mathbf{R} covariance matrices are diagonal matrices. By considering the following augmented state vector of dimension $\bar{n} = n + p_2$

$$\bar{\mathbf{x}} = \begin{bmatrix} \mathbf{x} \\ \mathbf{u}^* \end{bmatrix} \in \mathbb{R}^{\bar{n} \times 1} \quad (10)$$

the set of Equations (9) is rephrased as

$$\begin{cases} \dot{\bar{\mathbf{x}}} = \bar{\mathbf{A}}\bar{\mathbf{x}} + \bar{\mathbf{B}}\mathbf{u} + \bar{\mathbf{G}}\bar{\mathbf{w}} \\ \mathbf{y} = \bar{\mathbf{C}}\bar{\mathbf{x}} + \mathbf{D}\mathbf{u} + \mathbf{v} \end{cases} \quad (11)$$

with

$$\begin{aligned} \bar{\mathbf{A}} &= \begin{bmatrix} \mathbf{A} & \mathbf{B}^* \\ \mathbf{0} & \mathbf{0} \end{bmatrix} \in \mathbb{R}^{\bar{n} \times \bar{n}}, & \bar{\mathbf{B}} &= \begin{bmatrix} \mathbf{B} \\ \mathbf{0} \end{bmatrix} \in \mathbb{R}^{\bar{n} \times p_1}, \\ \bar{\mathbf{G}} &= \begin{bmatrix} \mathbf{G} & \mathbf{0} \\ \mathbf{0} & \mathbf{I} \end{bmatrix} \in \mathbb{R}^{\bar{n} \times \bar{n}}, & \bar{\mathbf{w}} &= \begin{bmatrix} \mathbf{w} \\ \mathbf{w}_{\mathbf{u}^*} \end{bmatrix} \in \mathbb{R}^{\bar{n}}, \\ \bar{\mathbf{C}} &= [\mathbf{C} \quad \mathbf{D}^*] \in \mathbb{R}^{m \times \bar{n}} \end{aligned}$$

The set of Equations (11) is again an LTI system. This holds even for other models that we may use to describe the unknown inputs, such as the almost constant rate model. Thus, the classical linear KF can be implemented, with all the advantages of that very efficient algorithm. Specifically, the observability of the system is checked by considering the following matrix

$$\mathbf{O} = \begin{bmatrix} \bar{\mathbf{C}} \\ \bar{\mathbf{C}}\bar{\mathbf{A}} \\ \vdots \\ \bar{\mathbf{C}}\bar{\mathbf{A}}^{\bar{n}-1} \end{bmatrix} \in \mathbb{R}^{m\bar{n} \times \bar{n}} \quad (12)$$

If the rank of the matrix Eq. (12) is equal to the augmented state vector dimension \bar{n} , the system may be observable, even though how much the system is effectively observable deserves to be further investigated, as discussed in the next section. For the sake of brevity, details on the well-known classical linear KF routine are omitted in this manuscript.

III. THE OBSERVABILITY PROBLEM

As shown in the previous section, the joint estimation of states and unknown inputs leads to the dynamical system Eq. (11) that is again an LTI system with an augmented state vector of dimension \bar{n} . Thus, the observability of such an augmented

system can be investigated as that of a classical LTI system but considering the new augmented matrices and vectors. For this kind of system, the rank of the matrix Eq. (12) provides a direct check of the observability. In fact, as said, the system is observable only if the rank equals the dimension \bar{n} of the augmented state vector, unobservable otherwise. However, even if the rank satisfies the said observability criterion, the so-called degree of observability also needs to be investigated, as we show by discussing the numerical results in Section IV. The degree of observability of dynamical systems has been studied during the last decades and it still represents an open research field. Among the existing approaches for evaluating the degree of observability, we here collect and rigorously discuss those afterwards implemented and exploited for the aims of the paper. We comment that most of the proposed methods for observability analysis appear scattered in the scientific literature and the lack of a manuscript collecting more approaches together is a further contribution provided by the present research. In this regard, we, here, present methods for checking the degree of observability of LTI dynamical systems, dedicated to the case of augmented state vectors with unknown inputs, that can be traced back to the SVD (Singular Value Decomposition) of matrix Eq. (12), referred to as the observability matrix, for the valuable information directly provided about the degree of observability of an LTI system. In fact, by considering, without loss of generality, the set of Eqs. (11) in the absence of known inputs

$$\begin{cases} \dot{\bar{\mathbf{x}}} = \bar{\mathbf{A}}\bar{\mathbf{x}} + \bar{\mathbf{G}}\bar{\mathbf{w}} \\ \mathbf{y} = \bar{\mathbf{C}}\bar{\mathbf{x}} + \mathbf{v} \end{cases} \quad (13)$$

it is possible to write the following set of holding equations

$$\begin{cases} \mathbf{y} = \bar{\mathbf{C}}\bar{\mathbf{x}} + \mathbf{v} \\ \dot{\mathbf{y}} = \bar{\mathbf{C}}\dot{\bar{\mathbf{x}}} + \dot{\mathbf{v}} = \bar{\mathbf{C}}\bar{\mathbf{A}}\bar{\mathbf{x}} + \bar{\mathbf{C}}\bar{\mathbf{G}}\bar{\mathbf{w}} + \dot{\mathbf{v}} \\ \ddot{\mathbf{y}} = \bar{\mathbf{C}}\bar{\mathbf{A}}^2\bar{\mathbf{x}} + \bar{\mathbf{C}}\bar{\mathbf{A}}\bar{\mathbf{G}}\bar{\mathbf{w}} + \bar{\mathbf{C}}\bar{\mathbf{G}}\dot{\bar{\mathbf{w}}} + \ddot{\mathbf{v}} \\ \vdots \\ \mathbf{y}^{(\bar{n}-1)} = \bar{\mathbf{C}}\bar{\mathbf{A}}^{\bar{n}-1}\bar{\mathbf{x}} + \sum_{q=0}^{\bar{n}-2} \bar{\mathbf{C}}\bar{\mathbf{A}}^{\bar{n}-2-q}\bar{\mathbf{G}}\bar{\mathbf{w}}^{(q)} + \mathbf{v}^{(\bar{n}-1)} \end{cases} \quad (14)$$

We comment that higher-order derivatives do not add information in compliance with the Cayley-Hamilton theorem. By rephrasing system (14) in the following compact form

$$\mathbf{y}^{(d)} = \mathbf{O}\bar{\mathbf{x}} + \mathbf{E} \quad (15)$$

and pre-multiplying by \mathbf{O}^T , we have

$$\mathbf{O}^T\mathbf{y}^{(d)} = \mathbf{O}^T\mathbf{O}\bar{\mathbf{x}} + \mathbf{O}^T\mathbf{E} \quad (16)$$

where the matrix $\mathbf{O}^T\mathbf{O} \in \mathbb{R}^{\bar{n} \times \bar{n}}$ is invertible if it has a full rank, equal to \bar{n} , proving the observability criterion for the

observability check exposed above. In this hypothesis

$$\bar{\mathbf{x}} = (\mathbf{O}^T \mathbf{O})^{-1} \mathbf{O}^T \mathbf{y}^{(d)} - (\mathbf{O}^T \mathbf{O})^{-1} \mathbf{O}^T \mathbf{E} = \mathbf{O}^\dagger \mathbf{y}^{(d)} - \mathbf{O}^\dagger \mathbf{E} \quad (17)$$

where $\mathbf{O}^\dagger \in \mathbb{R}^{\bar{n} \times m\bar{n}}$ is the Moore-Penrose pseudoinverse matrix of \mathbf{O} . Equation (17) splits the computed augmented states into actual states and a noise related error term. The actual states are a linear combination of the measurements. The error term is a linear combination of process and measurement noises instead. The check of the degree of observability can be performed by using \mathbf{O} or its pseudoinverse, and, thus, in terms of singular values and vectors of \mathbf{O} .

In a first possible approach, the usage of observability matrix \mathbf{O} is exploited, because it can be directly obtained by combining \mathbf{A} and \mathbf{C} matrices of the augmented state-space system. Since the observability criterium is based on the rank of \mathbf{O} that has to equal \bar{n} , one expects that \mathbf{O} has \bar{n} independent rows among the available $m\bar{n}$. Therefore, the degree of independency of these rows is also the degree of observability of the system [26]. In particular, if \bar{n} orthogonal rows of \mathbf{O} can be found, the system observability is as high as possible. On the other hand, if an orthogonal (or nearly orthogonal) vector with respect to all the $m\bar{n}$ rows of \mathbf{O} exists, the system is ill-conditioned because the determinant of a matrix obtained with any combination of the \bar{n} rows is rather small, i.e., all the rows of \mathbf{O} are nearly proportional. The direction of this vector provides information about the least observable states. Since the direction of the row vectors of \mathbf{O} is of interest, the observability matrix is first normalized with respect to its rows, leading to the normalized observability matrix \mathbf{O}_N . Therefore, a quadratic function L is introduced in order to find a vector $\boldsymbol{\chi}$ of unit length ($\boldsymbol{\chi}^T \boldsymbol{\chi} = 1$) being the “most orthogonal” with respect to the rows of matrix \mathbf{O}_N

$$L = \boldsymbol{\chi}^T (\mathbf{O}_N^T \mathbf{O}_N) \boldsymbol{\chi} \quad (18)$$

This represents the classical maxima-minima identification of a constrained problem that can be solved via the Lagrangian multipliers formulation, leading to the following well-known eigenvalues problem

$$(\mathbf{O}_N^T \mathbf{O}_N - \lambda \mathbf{I}) \boldsymbol{\chi} = \mathbf{0}; \quad (19)$$

From Equation (19), the “most orthogonal” vector is the eigenvector associated with the smallest eigenvalue, which leads to the minimum of the quadratic function L and provides the direction of the maximum error. The component of this eigenvector that contributes more to the direction of the maximum error is the largest one, associated with the least observable state variable. *Vice versa*, the smallest component of the eigenvector is associated with the most observable state.

A second possible approach relies on the usage of the pseudoinverse of normalized observability matrix \mathbf{O}_N^\dagger to investigate the degree of observability of each state.

In Equation (17), $\mathbf{O}^\dagger \mathbf{y}^{(d)}$ can be considered the actual state vector as if it was measured. Therefore, by rearranging this equation, the following error associated with the estimation process is obtained

$$\mathbf{O}^\dagger \mathbf{E} = \mathbf{O}^\dagger \mathbf{y}^{(d)} - \bar{\mathbf{x}} = \mathbf{e} \quad (20)$$

By considering the k -th state variable, Equation (20) becomes

$$\mathbf{O}^\dagger(k, :) \mathbf{E} = \mathbf{e}_k \quad (21)$$

where $\mathbf{O}^\dagger(k, :)$ indicates the k -th row of \mathbf{O}^\dagger . A reliable parameter associated with the degree of observability is the upper-bound error leading to the *upper-bound observability*, defined as

$$DO_{k,UP} = \frac{1}{\sum_{i=1}^{m\bar{n}} |m_{k,i}|} \quad (22)$$

where $m_{k,i}$ is the i -th entry in the k -th row of the matrix \mathbf{O}_N^\dagger . The lower the value of $DO_{k,UP}$, the lower the degree of observability of the k -th state. A formal derivation of Equation (22) is provided in Appendix A. Other parameters rely on the variance and the standard deviation of the error instead

$$DO_{k,var} = \frac{1}{\sum_{i=1}^{m\bar{n}} m_{k,i}^2} \quad (23)$$

$$DO_{k,std} = \sqrt{\frac{1}{\sum_{i=1}^{m\bar{n}} m_{k,i}^2}} \quad (24)$$

The *variance observability* $DO_{k,var}$ parameter is newly introduced in this paper (see Appendix B). Instead, the *standard-deviation observability* $DO_{k,std}$ parameter, equal to the square root of the previous one, can also be found in [26], together with $DO_{k,UP}$. The parameter $DO_{k,var}$ is also useful for investigating the matrix \mathbf{O}_N^\dagger in terms of its SVD

$$\mathbf{O}_N^\dagger = \mathcal{V} \mathcal{S}^\dagger \mathcal{U}^T = \sum_{i=1}^{\bar{n}} \sigma_i^{-1} \mathbf{v}_i \mathbf{v}_i^T \quad (25)$$

where \mathcal{U} and \mathcal{V} are the orthogonal matrices of left and right eigenvectors, \mathcal{S} is the rectangular matrix containing the singular values σ and \mathbf{v} and \mathbf{v} represent, respectively, the columns of the previous orthogonal matrices. Being the singular values numerically comparable, we observe that all of them contribute significantly to the matrix decomposition, and, thus, to the correct detection of the degree of observability of each state. In conclusion, the *variance observability* may be written as follows

$$DO_{k,var} = \left[\sum_{i=1}^{\bar{n}} \text{tr} \left(\sigma_i^{-2} v_{k,i}^2 \mathbf{v}(:, i) [\mathbf{v}(:, i)]^T \right) \right]^{-1} \quad (26)$$

where $v_{k,i}^2$ is the k -th element of the i -th column \mathbf{v}_i of matrix \mathcal{V} and tr indicates the trace operator.

The methods for checking the degree of observability presented above, do not suit estimators like GKF-UI, where the estimation of unknown states and inputs is performed with dedicated algorithms. The observability of these LTI systems has been widely investigated over the years, such as in [27], [28], [29], [30], [31], [32], [33], and [34]. The main concept is grounded on the following reasonable assumption: whenever the outputs, i.e. the measurements, of a generic LTI system are known but not the inputs, the invertibility of the system implies observability. As stated above, when the number of the measurements m is greater than the number of the unknown inputs p_2 , the system can be considered observable. Nevertheless, this condition behaves like the rank of the observability matrix Eq.(12) for the previous type of systems, and it might not be sufficient, as shown in Section IV. Further information about the observability can be provided by the Rosenbrock matrix [35] of system Eq. (1)

$$\mathfrak{R}(s) = \begin{bmatrix} s\mathbf{I} - \mathbf{A} & \mathbf{B}^* \\ \mathbf{C} & \mathbf{D}^* \end{bmatrix}$$

If the following condition holds

$$\forall s \in \mathbb{C} \mid \text{rank} [\mathfrak{R}(s)] = n + p_2 \quad (27)$$

the system is invertible and then observable. It may happen that the number of measurements m is greater than the number of unknown inputs p_2 , but the condition (27) is not satisfied. This means that the role played by some measurements may be more important than that played by others, as shown in the next sections.

IV. NUMERICAL RESULTS

In this section, we compare the estimation of road input and non-measurable states obtained by using the GKF-UI with that achieved by the joint estimation performed via AKF-UI, in terms of estimation accuracy and computational efficiency. At the same time, the role played by the considered measurements is investigated. First, albeit vector \mathbf{y} does not consider y_1 , the number of measurements is still greater than the unknown inputs because $m = 3$ and $p_2 = 1$, and therefore the system observability should be preserved. But the rank of the Rosenbrock matrix is less than $n + p_2$ without y_1 . In this research, the Rosenbrock matrix calculation is carried out with $s = 0$. Interestingly, we notice that by keeping y_1 and removing other measurements, such as $y_1 - y_2$, \dot{y}_1 , or both, the rank of the Rosenbrock matrix is preserved, and the observer works well. Of course, the number of measurements must be at least two to have $m > p_2$. However, although the observability is preserved, removing measurements from vector \mathbf{y} Eq. (4) leads to a biased estimate of the unknown input, that is the road profile, as displayed in Figure 2 and Figure 3. The GKF-UI-based observer stops working without y_1 regardless of the number of measurements considered. Figure 3 displays the error for different \mathbf{y} vectors in terms of bias and accuracy, respectively quantified by computing average value and standard deviation, with quantitative values reported in the captions.

By this example, we enlighten the fact that the input reconstruction is, de facto, unreachable when the measurement y_1 is not available, regardless of the number of direct measurements made on the system. This specific measurement can not be obtained directly in practice without the use of expensive devices.

Further analyses are carried out by exploiting the AKF-UI algorithm using the same measurement vectors above. As stated in Section II-B, this approach needs to define a model for the unknown input $\mathbf{u}^* = [h]$, for which a widely used model is, as said, a zero-mean zero-order random walk. The augmented state vector is

$$\bar{\mathbf{x}} = [y_1 \ y_2 \ \dot{y}_1 \ \dot{y}_2 \ h]^T \quad (28)$$

and the AKF-UI-based estimations are performed under the following assumptions

$$\mathbf{G} = \mathbf{I}_{\bar{n} \times \bar{n}}$$

$$\mathbf{Q} = \text{diag} [s_1^2 \ s_2^2 \ s_3^2 \ s_4^2 \ s_5^2]$$

$$\mathbf{R} = \text{diag} [r_1^2 \ r_2^2 \ r_3^2 \ r_4^2]$$

$$\bar{\mathbf{x}}_{0|0} = \mathcal{N}(\mathbf{0}, 10^{-4} \cdot \mathbf{I}_{\bar{n} \times \bar{n}})$$

$$\mathbf{P}_{0|0} = \text{diag} [10^2 \ 10^2 \ 10^2 \ 10^2 \ 10^3]$$

with $\bar{n} = 5$, s_k is the standard deviation of the k -th state variable, and r_i is the standard deviation of the i -th measurement. For the system under consideration, we assume uncolored process noise and no correlation among states, resulting in \mathbf{G} being an identity matrix. The initial state is set to the zero vector since we are processing vibrations, while the initial state-error covariance matrix $\mathbf{P}_{0|0}$ is considered high due to the low confidence assigned to the first step of the estimation routine, particularly for the last state, which is the most challenging. Finally, the \mathbf{Q} and \mathbf{R} matrices, representing the process and measurement noise covariances respectively, are tuned via a trial-and-error procedure based on the physical understanding of the problem. Their values are collected in Table 5 in Appendix C, along with the QC system parameters. It is worth pointing out that the initial variance of the 5th state variable is greater than that of the other states due to the absence of an *a priori* known model of h . At the same time, the variance of the sprung mass displacement measurement y_1 is low since it would represent the most reliable measurement. The variance associated with the accelerations is selected higher than the variance of the sensors' noise to consider the effect of the unmodelled phenomena.

For the case of h modelled as a random walk, the following augmented state evolution (process) matrix is considered

$$\bar{\mathbf{A}} = \begin{bmatrix} \mathbf{A} & \mathbf{B}^* \\ \mathbf{0} & \mathbf{0} \end{bmatrix} \quad (29)$$

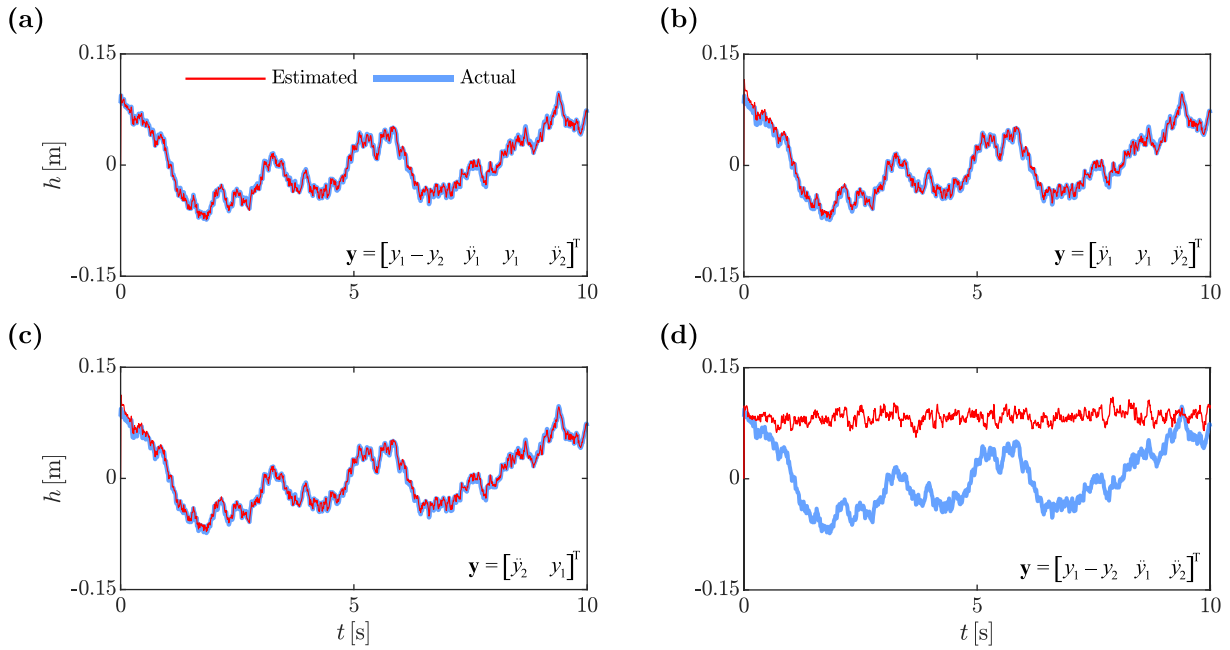


FIGURE 2. Road profile estimation for different measurement vectors and GKF-UI algorithm.

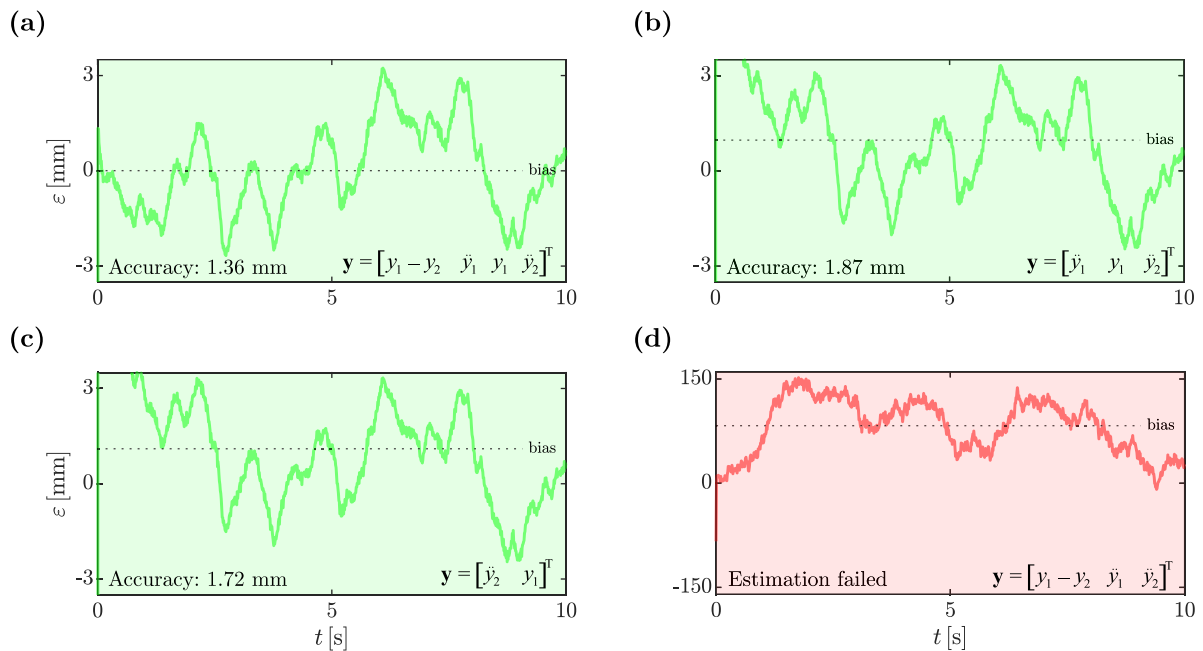


FIGURE 3. Error in road profile estimate for different measurement vectors and GKF-UI algorithm.

The results reflect those achieved with the previous approach, even though this method appears slightly more robust. In fact, by reducing the number of measurements in vector \mathbf{y} , the accuracy of the estimation does not deteriorate and remains unbiased, as displayed in Figure 4. Moreover, the error in road input estimation is more similar to white noise if compared with the previous case, and this represents a further checking of the goodness of the estimator. Nonetheless,

without the (not directly available in practice) measurement of the sprung mass displacement y_1 , the estimation fails again. It is worth highlighting that when the system loses observability, the minimum eigenvalue λ_{min} is basically vanishing, as reported in the caption of Figure 4. Therefore, the higher the value of λ_{min} , the more observable the system is. As expected, the more measurements, the more observable the system is, since the higher λ_{min} . The value

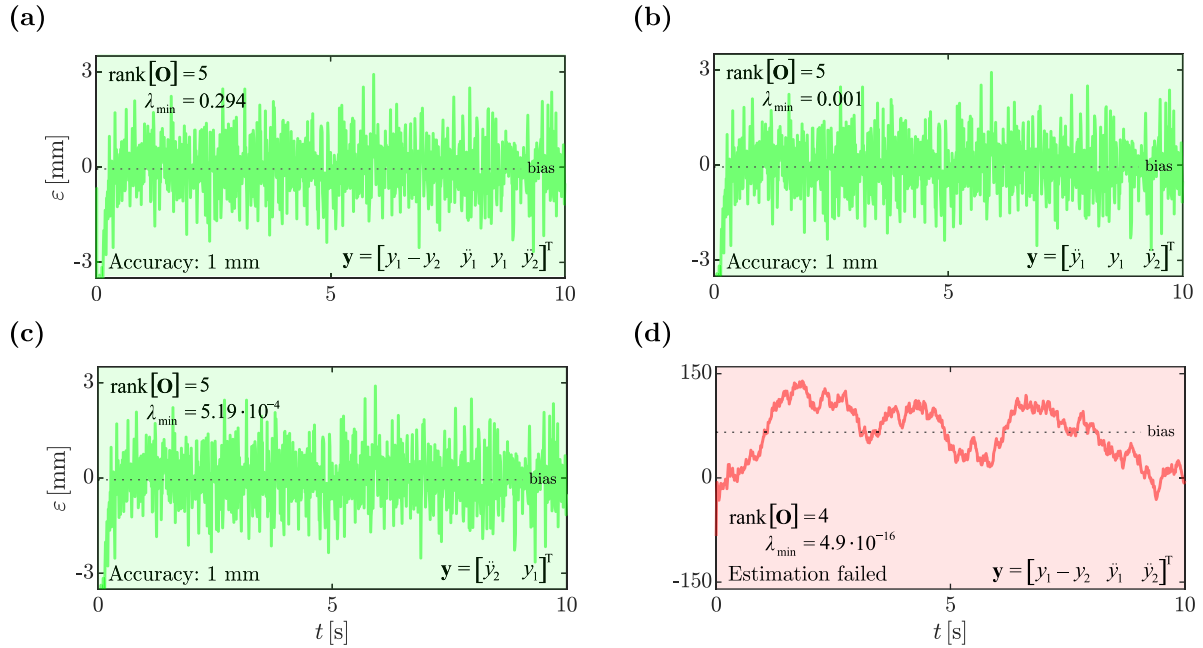


FIGURE 4. Error in road profile estimate for different measurement vectors, AKF-UI algorithm, and unknown input h modelled as a random walk.

TABLE 1. Degree of observability of the states for different measurement vectors.

\bar{x}	$\mathbf{y} = [y_1 - y_2 \quad \dot{y}_1 \quad y_1 \quad \ddot{y}_2]^T$			$\mathbf{y} = [\dot{y}_1 \quad y_1 \quad \ddot{y}_2]^T$			$\mathbf{y} = [y_1 \quad \ddot{y}_2]^T$		
	χ_k	$DO_{k,up}$	$DO_{k,var}$	χ_k	$DO_{k,up}$	$DO_{k,var}$	χ_k	$DO_{k,up}$	$DO_{k,var}$
y_1	0.0261	1.000	2.000	0.00008	1.000	2.000	0.00004	1.000	2.000
y_2	0.0710	0.398	1.104	0.0793	0.125	0.136	0.0792	0.118	0.069
\dot{y}_1	0.3806	0.924	1.001	0.0001	0.994	1.000	0.00006	0.997	1.000
\dot{y}_2	0.9181	0.342	0.336	0.9934	0.014	0.001	0.9935	0.013	0.0005
h	0.0808	0.236	0.801	0.0832	0.111	0.119	0.0816	0.109	0.061

of λ_{min} also represents a first check of the degree of observability.

The degree of observability is now investigated by exploiting the methods explained in Section III. In this research, the knowledge of the contribution of the y_1 measurement is of interest, as said. In Table 1, we list the degree of observability in three different cases related to the three different vectors \mathbf{y} considered and for three different approaches: the most orthogonal unit vector χ with respect to the rows of the matrix \mathbf{O}_N , the upper-bound observability and the variance observability. As expected, all methods lead to the same conclusion: the most observable state is y_1 , because it is “measured directly”. In fact, the upper-bound error of the first state estimation is the same as the measurement upper-bound error, and the variance is half instead. The first element of the unit vector χ , associated with the first state, is the one that contributes less to system ill-conditioning. This is particularly true when the number of measurements

decreases. Interestingly, a similar role is also played by the second state variable, i.e., the sprung mass velocity \dot{y}_1 .

By considering reasonable assumptions about the road profile geometry, similar to those adopted in Refs. [23] and [24], we account for the following first-order random walk model type

$$\dot{h}(t) = -\alpha h(t) + \beta w(t) \tag{30}$$

where α and β are constant coefficients and $w(t)$ is a zero-mean Gaussian white noise process. Equation (30) represents an *a priori* known model. Since we are interested in observability recovery, without loss of generality, we assume for simplicity $\alpha = 1$, achieving the following augmented state-space (process) matrix

$$\bar{\mathbf{A}} = \begin{bmatrix} \mathbf{A} & \mathbf{B}^* \\ \mathbf{0} & \mathbf{I} \end{bmatrix} \tag{31}$$

TABLE 2. Comparison between the two AKF-UI-based observers.

AKF-UI with zero-order random walk				
\mathbf{y}	rank[O]	λ_{min}	bias [mm]	accuracy [mm]
$\mathbf{y} = [y_1 - y_2 \quad \ddot{y}_1 \quad y_1 \quad \ddot{y}_2]^T$	5	0.2937	x	1
$\mathbf{y} = [\ddot{y}_1 \quad y_1 \quad \ddot{y}_2]^T$	5	0.0010	x	1
$\mathbf{y} = [y_1 \quad \ddot{y}_2]^T$	5	$5.19 \cdot 10^{-4}$	x	1
$\mathbf{y} = [y_1 - y_2 \quad \ddot{y}_1 \quad \ddot{y}_2]^T$	4	$4.9 \cdot 10^{-16}$	fail	fail
AKF-UI with first-order random walk				
\mathbf{y}	rank[O]	λ_{min}	bias [mm]	accuracy [mm]
$\mathbf{y} = [y_1 - y_2 \quad \ddot{y}_1 \quad y_1 \quad \ddot{y}_2]^T$	5	0.2938	x	1
$\mathbf{y} = [\ddot{y}_1 \quad y_1 \quad \ddot{y}_2]^T$	5	0.0012	x	1
$\mathbf{y} = [y_1 \quad \ddot{y}_2]^T$	5	$5.95 \cdot 10^{-4}$	x	1
$\mathbf{y} = [y_1 - y_2 \quad \ddot{y}_1 \quad \ddot{y}_2]^T$	5	$1.1 \cdot 10^{-8}$	fail	fail

TABLE 3. Degree of observability without y_1 in the measurement vector for the AKF-UI-based estimator with h modelled with the identity.

$\bar{\mathbf{x}}$	χ	$DO_{k,up}$	$DO_{k,var}$
y_1	0.4486	$7.9 \cdot 10^{-4}$	$5.5 \cdot 10^{-7}$
y_2	0.4486	$7.9 \cdot 10^{-4}$	$5.5 \cdot 10^{-7}$
\dot{y}_1	0.4451	$8.0 \cdot 10^{-4}$	$5.6 \cdot 10^{-7}$
\dot{y}_2	0.4451	$8.0 \cdot 10^{-4}$	$5.6 \cdot 10^{-7}$
h	0.4486	$7.9 \cdot 10^{-4}$	$5.5 \cdot 10^{-7}$

with $\mathbf{I} = [1]$, obtaining results similar to those of the previous case, as listed in Table 2. Parameter β is included within matrix \mathbf{G} and acts as a tuning parameter for the KF. Again, without measuring the sprung mass displacement, or any other direct state, the system is not observable. In this latter case, we interestingly note that the rank of the observability matrix is full-column, as highlighted in Table 2. Nevertheless, the observer fails the estimation because the degree of observability is not sufficient. The degree of observability has been investigated as in the previous case and results are collected in Table 3. The minimum eigenvalue is rather small, and all the components of the unit vector χ provide the same contribution to the ill-conditioned problem. Furthermore, all the values of the upper-bound observability and the variance observability are too small, indicating that the error state estimation is much greater than the measurement error.

At last, we comment that the AKF-UI algorithm is much lighter than the GKF-UI one in terms of computational effort, as expected. In fact, the AKF-UI algorithm is actually a classical linear KF, which is a very efficient routine. Nonetheless, we, here, provide a novel side-by-side

comparison. Figure 5 displays the time (in [ms]) required for each step of the estimation routine performed with the GKF-UI algorithm (solid grey line) and with the AKF-UI one (solid black line). The average time required for one step was 4.79 ms for the GKF-UI and 0.03 ms for the AKF-UI, about 160 times lower. The estimation algorithms have been performed with an Intel(R) Core(TM) i7-8550U CPU @ 1.80GHz, running the software *Matlab* R2022a.

V. EXPERIMENTAL RESULTS

To provide a complete picture of the problem, the experimental setup depicted in Figure 6 (a) is appropriately designed for this research. The system consists of two plates joined together by four springs. The unsprung mass is connected via four springs to another plate bolted to the electrodynamic shaker *Dongling ES-2-150*. The idea is to simulate a two Degrees Of Freedom (DOFs) system like the QC model, with two masses, a suspension system and the tire. The input to the system is provided by the shaker driven through an acceleration signal-controlled closed loop via an electric input signal generated with an *LMS SCADAS 310* mobile PC-based multichannel analyzer platform, running the *Siemens LMS Test.Lab 14A* software suite, using the measure obtained by a triaxial accelerometer *B&K 4535-B-001* rigidly connected to the vibrating plate bolted to the shaker. The input is forced to follow the design acceleration spectrum shown in Figure 6 (b), which is thought to provide a displacement spectrum similar to that of a generic road profile. The outputs are the two accelerations measured at the Center of Gravity (CoG) of the two masses and the velocity and the displacement of the sprung mass measured by using the *Polytec OFV-5000* modular LD vibrometer with a laser beam pointed towards the centre of the plate.

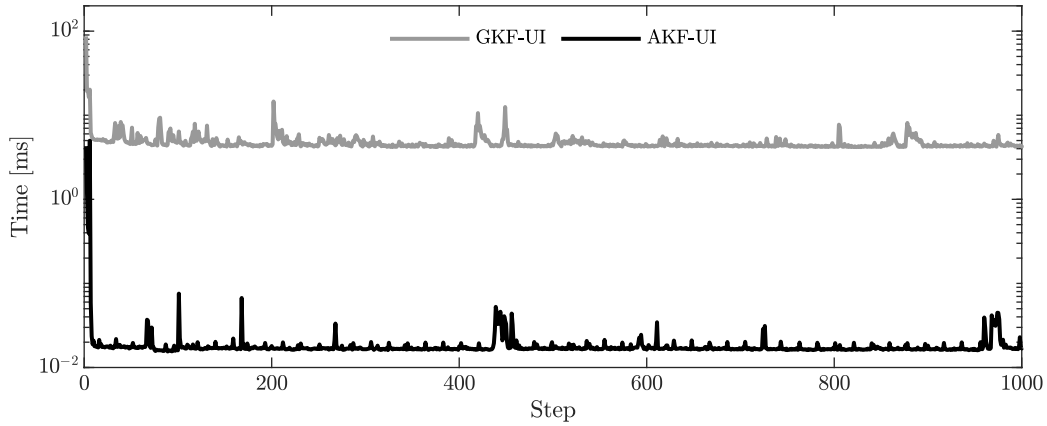


FIGURE 5. Time required for each step of GKF-UI routine (grey line) and AKF-UI one (black line).

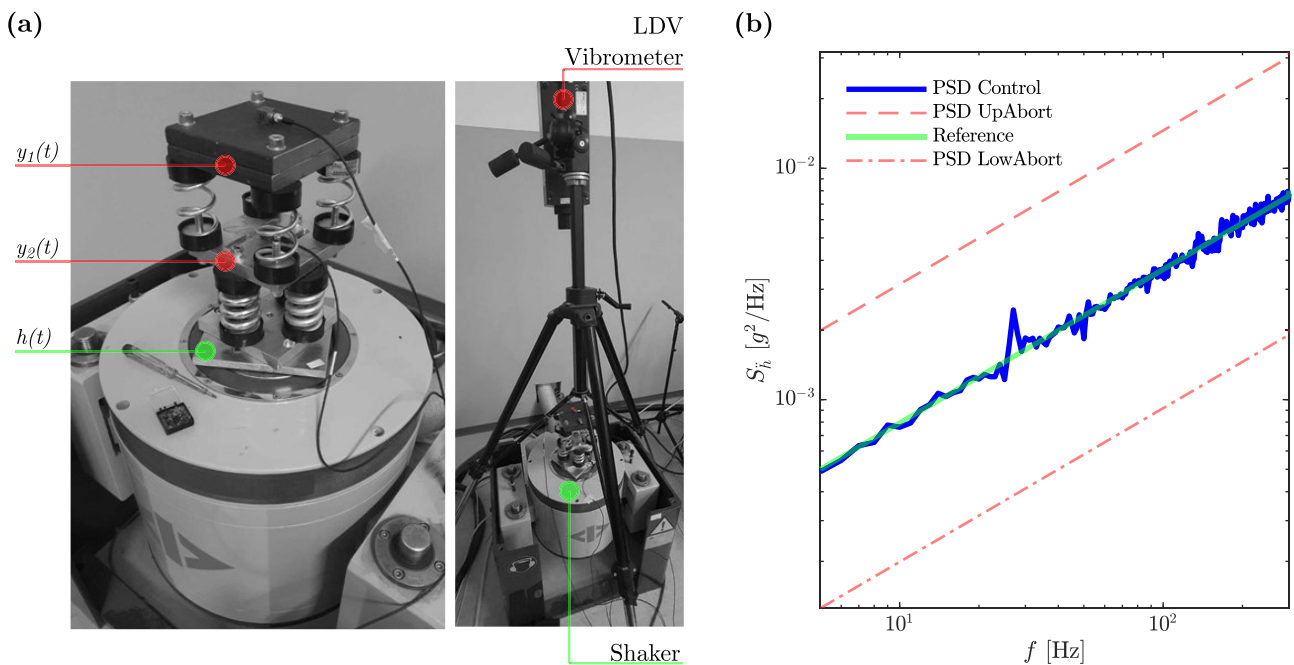


FIGURE 6. (a) The experimental setup exploited in this research. On the right, the entire system, consisting of the shaker, the laser-Doppler vibrometer mounted on a tripod and the mechanical system. The mechanical system is highlighted on the left, along with the accelerometers. (b) PSD Average Control.

TABLE 4. Results of the observability analysis conducted on the experimental setup.

\mathbf{y}	$\text{rank}[\Re(s)]$	$\text{rank}[\mathbf{O}]$	λ_{\min}	Most observable state
$\mathbf{y} = [y_1 - y_2 \quad \ddot{y}_1 \quad y_1 \quad \ddot{y}_2]^T$	5	5	$5.38 \cdot 10^{-4}$	1°
$\mathbf{y} = [\ddot{y}_1 \quad y_1 \quad \ddot{y}_2]^T$	5	5	$2.95 \cdot 10^{-4}$	1°
$\mathbf{y} = [y_1 \quad \ddot{y}_2]^T$	5	5	$1.87 \cdot 10^{-4}$	1°
$\mathbf{y} = [y_1 - y_2 \quad \ddot{y}_1 \quad \ddot{y}_2]^T$	4	4	$2.15 \cdot 10^{-16}$	fail

Before dealing with the observability analysis, the system is identified. Figure 7 (a) displays the Frequency Response Functions (FRFs) of the experimental system at hand in

the frequency band of interest, with highlighted the natural frequencies. The blue line is the FRF between sprung mass acceleration and input acceleration, and the red line is the

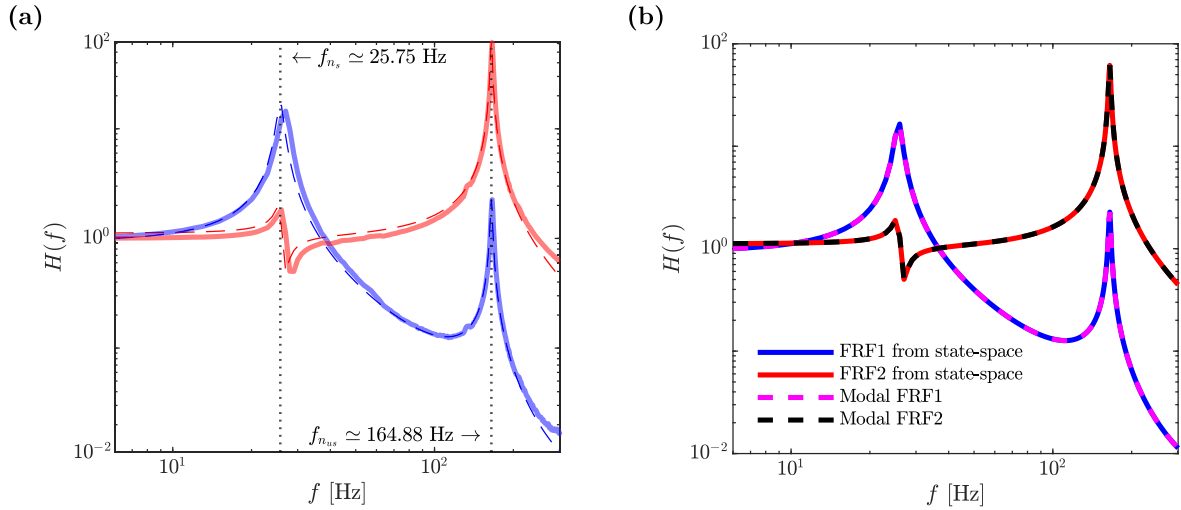


FIGURE 7. (a) FRFs provided by Siemens Test.Lab software (solid lines) and synthesized FRFs from modal parameters (dashed lines). (b) FRFs of the experimental setup.

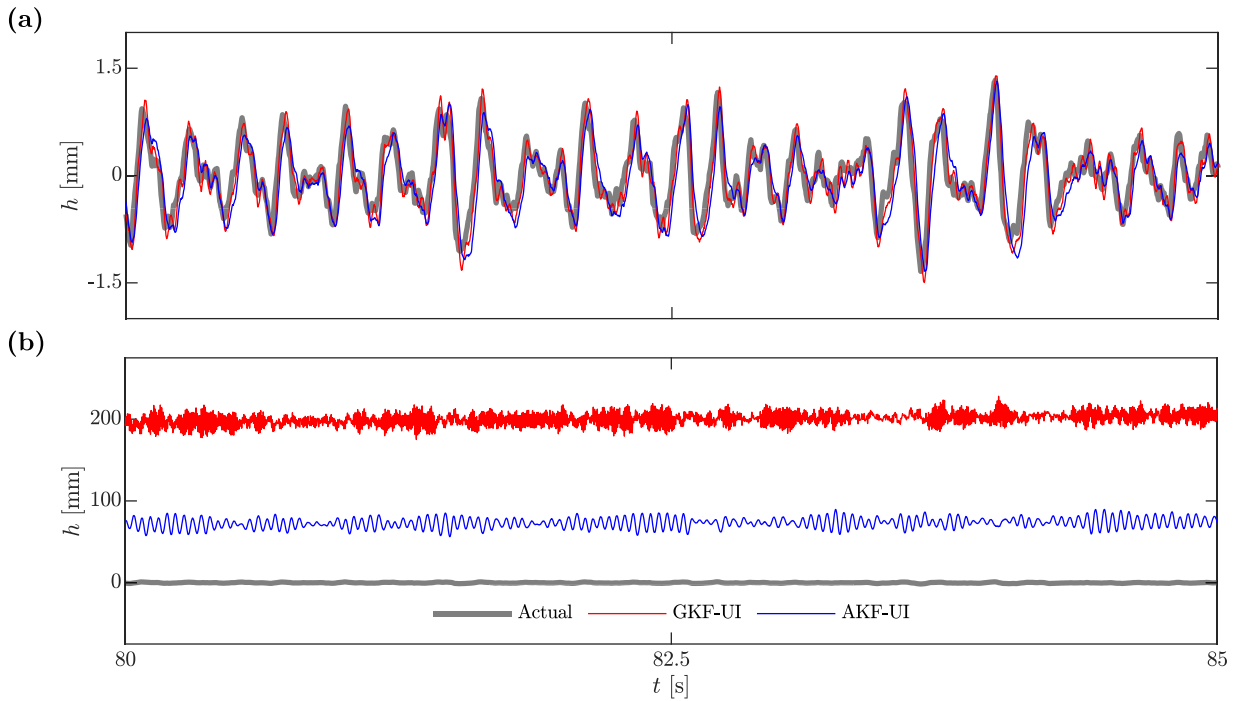


FIGURE 8. Input reconstruction by using the GKF-UI (red line) and the AKF-UI (blue line) in both the observable (top) and the unobservable case (bottom).

FRF related to the unsprung mass. Solid lines are the FRFs directly provided by the software for modal analysis *Siemens Test.Lab*, and the dashed lines are the synthesized FRFs obtained from modal parameters

$$\mathbf{H}(i\omega) = \boldsymbol{\psi} (i\omega\mathbf{I} - \boldsymbol{\Lambda})^{-1} \mathbf{L} \quad (32)$$

where $\boldsymbol{\psi}$ is the matrix of modal vectors, $\boldsymbol{\Lambda}$ is the diagonal matrix of the system eigenvalues and \mathbf{L} is the modal participation factor matrix. Since the following equations hold

$$\mathbf{A} = \boldsymbol{\psi} \boldsymbol{\Lambda} \boldsymbol{\psi}^{-1}$$

$$\mathbf{B} = \boldsymbol{\psi} \mathbf{L}$$

$$\mathbf{C} = \begin{bmatrix} 1 & 0 & 0 & 0 \\ 0 & 1 & 0 & 0 \end{bmatrix} \quad (33)$$

$$\mathbf{H}(i\omega) = \mathbf{C} (i\omega\mathbf{I} - \mathbf{A})^{-1} \mathbf{B} \quad (34)$$

one obtains the system in its continuous-time state-space representation. Results are displayed in Figure 7 (b). Refer to Appendix D for numerically evaluated state-space matrices. The ratio between accelerations leads to the system's transmissibility. Therefore, states are displacements and velocities of the two masses. It is also worth highlighting that the system

has 2 DOFs in the considered frequency range. In Table 4, we list results from the observability analysis performed on this system using the same vectors of measurements considered in the previous example. The velocity and the displacement of the input and the unsprung mass are obtained via numerical integration of the acceleration signals, with null initial conditions. The results agree with those obtained from the numerical example. As expected, the degree of observability is slightly reduced due to the unmodeled phenomena, which are non-existent for the simulated case. This aspect, in turn, affects the estimation accuracy. Finally, for the sake of completeness, the input reconstruction is displayed in Figure 8.

VI. CONCLUSION

In this paper, we have focused on estimating unknown inputs and states of dynamical systems, in the context of road profiles' reconstruction and vehicle dynamics identification. Two distinct Kalman filter (KF)-based observers have been applied to a 2-degree-of-freedom system, and a comprehensive a novel side-by-side comparison has highlighted their performance in terms of accuracy, robustness, and computational efficiency.

The study has revealed that the joint estimation approach, which involves augmenting the state vector with the unknown road profile input, outperforms a dedicated KF-based algorithm for linear time-invariant systems with unknown inputs. This better result is related to the improved quality of the estimation and to a reduced computational burden. Additionally, the joint estimation method has more effectively highlighted the importance of measurements in ensuring system observability. This approach has facilitated a deeper investigation through various parameters related to the degree of observability. Specifically, this research has gathered different methods scattered in the scientific literature and has introduced the concept of *variance observability*, exploring its relationship with the normalized observability matrix through its Singular Value Decomposition.

By using detailed mathematical explanations, we have shown that in the absence of a specific measurement, not readily available in practical scenarios, the system lacks sufficient observability, hindering the estimation process. Intriguingly, this missing measurement ends to be, actually, a state that cannot be directly measured without the use of expensive sensors. We have observed that a directly measured state may improve the observability of any dynamical system owing to the particular structure of the measurement matrix, which includes a canonical row. Accounting for all these factors, we conclude that the problem of road input estimation using KF-based observers may still be in need of a practical solution at least with a model-based observer grounded on the quarter-car. Future directions, thus, aim to investigate this topic by exploiting more sophisticated vehicle models with a higher number of degrees of freedom, to capture phenomena related to multi-input excitation.

DECLARATION OF COMPETING INTEREST

The authors declare that they have no known competing financial interests or personal relationships that could have appeared to influence the work reported in this article.

APPENDIX A

DERIVATION OF THE UPPER-BOUND OBSERVABILITY

In this appendix, the derivation of Equation (22) is provided. First, the ratio between the expected value of the difference between measured k -th state and the k -th state \mathbf{e}_k and the expected value of the error in the estimation process of the k -th state $\mathbf{O}^\dagger(k, :)\mathbf{E}$ is considered

$$DO_k = \frac{E[\mathbf{e}_k]}{E[m_{k,1}\mathbf{E}_1 + \dots + m_{k,m\bar{n}}\mathbf{E}_{m\bar{n}}]}$$

An unbiased estimator has an expected value of the errors equal to zero, therefore $E[\mathbf{e}_k] = E[\mathbf{E}_1] = \dots = E[\mathbf{E}_k] = \dots = E[\mathbf{E}_{m\bar{n}}] = 0$. Thus, the previous equation becomes

$$DO_k = \lim_{E[\mathbf{e}_k] \rightarrow 0} \left[\frac{E[\mathbf{e}_k]}{(m_{k,1} + \dots + m_{k,m\bar{n}}) E[\mathbf{e}_k]} \right] = \frac{1}{\sum_{i=1}^{m\bar{n}} m_{k,i}} \quad (35)$$

and since the maximum error is considered (the upper bound), the absolute value of every $m_{k,i}$ is taken in Equation (35).

APPENDIX B

DERIVATION OF THE VARIANCE OBSERVABILITY

By considering the k -th state with orthogonal uncertainties and for an unbiased estimator

$$\begin{aligned} E \left[\left(\mathbf{O}^\dagger(k, :)\mathbf{E} \right) \left(\mathbf{O}^\dagger(k, :)\mathbf{E} \right)^T \right] &= E[\mathbf{e}_k \mathbf{e}_k^T] \iff \\ \iff \mathbf{O}^\dagger(k, :)\text{Var}[\mathbf{E}] \left(\mathbf{O}^\dagger(k, :)\right)^T &= \text{Var}[\mathbf{e}_k] \end{aligned}$$

with $\text{Var}[\mathbf{E}]$ diagonal matrix due to the orthogonality. Since the error in the System (14) does not stack between two consecutive derivatives, one can put $\text{Var}[\mathbf{E}_1] = \dots = \text{Var}[\mathbf{E}_{m\bar{n}}] = \text{Var}[\boldsymbol{\xi}]$ and thus

$$DO_k = \frac{1}{\sum_{i=1}^{m\bar{n}} m_{k,i}^2} \frac{\text{Var}[\mathbf{e}_k]}{\text{Var}[\boldsymbol{\xi}]} \quad (36)$$

For a well-designed estimator, the error on the measured state is similar to the error on the estimated state, thus

$$\text{Var}[\mathbf{e}_k] \approx \text{Var}[\boldsymbol{\xi}]$$

therefore, the variance observability of Equation (23) is obtained. The standard-deviation observability is just the square root of $DO_{k,\text{var}}$.

APPENDIX C

TABLE OF QUANTITIES OF INTEREST

The table below is provided for any interested reader who wants to replicate the results.

TABLE 5. QC system and KF tuning parameters.

Parameter	Symbol	Value	Dimension
Sprung mass	m_s	455	kg
Unsprung mass	m_u	45.5	kg
Suspension stiffness	k	25	kN/m
Suspension damping	c	2	kNs/m
Tire stiffness	k_t	175	kN/m
1st state std	s_1	10^{-3}	m
2nd state std	s_2	10^{-3}	m/s
3rd state std	s_3	10^{-3}	m
4th state std	s_4	10^{-3}	m/s
5th state std	s_5	10^{-1}	m
Sprung mass displacement measurement std	r_1	10^{-6}	m
Suspension travel measurement std	r_2	10^{-1}	m
Sprung mass acceleration measurement std	r_3	2	m/s ²
Unsprung mass acceleration measurement std	r_4	2	m/s ²

APPENDIX D
STATE-SPACE MATRICES OF THE EXPERIMENTAL SYSTEM

$$A = \begin{bmatrix} 0 & 0 & 1 & 0 \\ 0 & 0 & 0 & 1 \\ -2.9339 \cdot 10^4 & 3.8377 \cdot 10^4 & -8.0993 & 0.5268 \\ 8.5897 \cdot 10^4 & -1.0701 \cdot 10^4 & -26.7334 & -18.2833 \end{bmatrix} \quad (37)$$

$$B = \begin{bmatrix} -11.9720 \\ 21.5983 \\ -1.4975 \cdot 10^4 \\ 1.1123 \cdot 10^6 \end{bmatrix} \quad (38)$$

REFERENCES

[1] J. Caroux, C. Lamy, M. Basset, and G.-L. Gissinger, "Sideslip angle measurement, experimental characterization and evaluation of three different principles," *IFAC Proc. Volumes*, vol. 40, no. 15, pp. 505–510, 2007.

[2] L. Boillereaux and J.-M. Flaus, "A new approach for designing model-based indirect sensors," *IEEE Trans. Control Syst. Technol.*, vol. 8, no. 4, pp. 601–608, Jul. 2000.

[3] G. Reina, A. Leanza, and G. Mantriota, "Model-based observers for vehicle dynamics and tyre force prediction," *Vehicle Syst. Dyn.*, vol. 60, no. 8, pp. 2845–2870, Aug. 2022.

[4] S.-W. Kang, J.-S. Kim, and G.-W. Kim, "Road roughness estimation based on discrete Kalman filter with unknown input," *Vehicle Syst. Dyn.*, vol. 57, no. 10, pp. 1530–1544, 2019.

[5] S. Pan, H. Su, J. Chu, and H. Wang, "Applying a novel extended Kalman filter to missile–target interception with APN guidance law: A benchmark case study," *Control Eng. Pract.*, vol. 18, no. 2, pp. 159–167, Feb. 2010.

[6] J. N. Yang, S. Pan, and H. Huang, "An adaptive extended Kalman filter for structural damage identifications II: Unknown inputs," *Structural Control Health Monitor.*, vol. 14, no. 3, pp. 497–521, 2007.

[7] M. Lungu and R. Lungu, "Full-order observer design for linear systems with unknown inputs," *Int. J. Control*, vol. 85, no. 10, pp. 1602–1615, Oct. 2012.

[8] H. E. Emará-Shabaik, "Filtering of linear systems with unknown inputs," *J. Dyn. Syst., Meas., Control*, vol. 125, no. 3, pp. 482–485, Sep. 2003.

[9] S. Gillijns and B. De Moor, "Unbiased minimum-variance input and state estimation for linear discrete-time systems," *Automatica*, vol. 43, no. 1, pp. 111–116, Jan. 2007.

[10] K. E. Fitch and H. J. Palanthandalam-Madapusi, "Unbiased minimum-variance filtering for delayed input reconstruction," in *Proc. Amer. Control Conf.*, Jun. 2011, pp. 4859–4860.

[11] C. Göhrle, A. Schindler, A. Wagner, and O. Sawodny, "Road profile estimation and preview control for low-bandwidth active suspension systems," *IEEE/ASME Trans. Mechatronics*, vol. 20, no. 5, pp. 2299–2310, Oct. 2015.

[12] G.-W. Kim, S.-W. Kang, J.-S. Kim, and J.-S. Oh, "Simultaneous estimation of state and unknown road roughness input for vehicle suspension control system based on discrete Kalman filter," *Proc. Inst. Mech. Eng. D, J. Automobile Eng.*, vol. 234, no. 6, pp. 1610–1622, May 2020.

[13] M. Doumiati, A. Victorino, A. Charara, and D. Lechner, "Estimation of road profile for vehicle dynamics motion: Experimental validation," in *Proc. Amer. Control Conf.*, Jun. 2011, pp. 5237–5242.

[14] W. Fauriat, C. Mattrand, N. Gayton, A. Beakou, and T. Cembrzynski, "Estimation of road profile variability from measured vehicle responses," *Vehicle Syst. Dyn.*, vol. 54, no. 5, pp. 585–605, May 2016.

[15] F. Yu and D. A. Crolla, "State observer design for an adaptive vehicle suspension," *Vehicle Syst. Dyn.*, vol. 30, no. 6, pp. 457–471, Dec. 1998.

[16] C.-S. Hsieh, "Robust two-stage Kalman filters for systems with unknown inputs," *IEEE Trans. Autom. Control*, vol. 45, no. 12, pp. 2374–2378, Dec. 2000.

[17] F. B. Hmida, K. Khémiri, J. Ragot, and M. Gossa, "Three-stage Kalman filter for state and fault estimation of linear stochastic systems with unknown inputs," *J. Franklin Inst.*, vol. 349, no. 7, pp. 2369–2388, Sep. 2012.

[18] S. Pan, P. Du, Y. Li, Z. Chen, and H. Wang, "The study on an general Kalman filter with unknown inputs," in *Proc. 11th World Congr. Intell. Control Autom.*, Jun. 2014, pp. 3562–3567.

[19] J. Y. Keller and M. Darouach, "Two-stage Kalman estimator with unknown exogenous inputs," *Automatica*, vol. 35, no. 2, pp. 339–342, Feb. 1999.

[20] D. Ichalal, B. Marx, J. Ragot, and D. Maquin, "Simultaneous state and unknown inputs estimation with PI and PMI observers for Takagi sugeno model with unmeasurable premise variables," in *Proc. 17th Medit. Conf. Control Autom.*, Jun. 2009, pp. 353–358.

- [21] S. S. Delshad, A. Johansson, M. Darouach, and T. Gustafsson, "Robust state estimation and unknown inputs reconstruction for a class of nonlinear systems: Multiobjective approach," *Automatica*, vol. 64, pp. 1–7, Feb. 2016.
- [22] A. F. Villaverde, N. Tsiantis, and J. R. Banga, "Full observability and estimation of unknown inputs, states and parameters of nonlinear biological models," *J. Roy. Soc. Interface*, vol. 16, no. 156, Jul. 2019, Art. no. 20190043.
- [23] G. Rill, *Road Vehicle Dynamics: Fundamentals and Modeling*. Boca Raton, FL, USA: CRC Press, 2011.
- [24] W. Chen, H. Xiao, Q. Wang, L. Zhao, and M. Zhu, *Integrated Vehicle Dynamics and Control*. Hoboken, NJ, USA: Wiley, 2016.
- [25] S.-J. Baek, B. R. Hunt, E. Kalnay, E. Ott, and I. Szunyogh, "Local ensemble Kalman filtering in the presence of model bias," *Tellus A, Dyn. Meteorol. Oceanogr.*, vol. 58, no. 3, pp. 293–306, Jan. 2006.
- [26] A. J. Marques, "On the relative observability of a linear system," Nav. Postgraduate School, Monterey, CA, USA, Tech. Rep. DTIC_ADA176772, 1986.
- [27] M. Hou and R. J. Patton, "Input observability and input reconstruction," *Automatica*, vol. 34, no. 6, pp. 789–794, Jun. 1998.
- [28] P. Kudva, N. Viswanadham, and A. Ramakrishna, "Observers for linear systems with unknown inputs," *IEEE Trans. Autom. Control*, vol. AC-25, no. 1, pp. 113–115, Jan. 1980.
- [29] L. Fridman, A. Levant, and J. Davila, "Observation of linear systems with unknown inputs via high-order sliding-modes," *Int. J. Syst. Sci.*, vol. 38, no. 10, pp. 773–791, Oct. 2007.
- [30] P. Moylan, "Stable inversion of linear systems," *IEEE Trans. Autom. Control*, vol. AC-22, no. 1, pp. 74–78, Feb. 1977.
- [31] R. Mohajerpoor, H. Abdi, and S. Nahavandi, "On unknown-input functional observability of linear systems," in *Proc. Amer. Control Conf. (ACC)*, Jul. 2015, pp. 3534–3539.
- [32] M. L. J. Hautus, "Strong detectability and observers," *Linear Algebra Appl.*, vol. 50, pp. 353–368, Apr. 1983.
- [33] S. Sefati, N. J. Cowan, and R. Vidal, "Linear systems with sparse inputs: Observability and input recovery," in *Proc. Amer. Control Conf. (ACC)*, Jul. 2015, pp. 5251–5257.
- [34] J. Kurek, "Observation of the state vector of linear multivariable systems with unknown inputs," *Int. J. Control*, vol. 36, no. 3, pp. 511–515, Sep. 1982.
- [35] W. Wolovich, "State-space and multivariable theory," *IEEE Trans. Autom. Control*, vol. AC-17, no. 4, pp. 583–584, Aug. 1972.



LEONARDO SORIA was born in Bari, Italy, in 1970. He received the M.S. degree in mechanical engineering and the Ph.D. degree in advanced production systems engineering from the Politecnico di Bari, Bari, in 1997 and 2003, respectively. His Ph.D. research concerning the role of multibody system dynamics in the functional design of mechanical devices. From 2004 to 2018, he was a tenured Assistant Professor of applied mechanics with the Politecnico di Bari, where he

has been an Associate Professor of applied mechanics with the Department of Mechanics, Mathematics, and Management, since 2019. He has been the Head of the Noise and Vibration Laboratory (NVLab), for about 20 years. In 2000, he won a Ph.D. Scholarship. He is the author of overall about 60 publications, of which three are international journal articles and one invention, of which he holds three national patents (Japan, China, and Europe). The teaching activity is spent on the courses of applied mechanics, mechanics of vibrations, and linear and nonlinear identification of mechanical vibrating systems. He has been the supervisor of about 200, among bachelor's and master's degree students and for about ten doctoral theses. He is a Founding Member of OMNIGRASP, a spin-off company of Politecnico di Bari. He has been involved in several research projects funded by the Italian Ministry for University and Research and the Apulia Region Administration, where he has been the coordinator for several research lines, as in international cooperation activities with foreign universities and industrial partners. His main research interests include noise and vibration engineering, including the dynamic identification and monitoring of systems, with specific focus on road and rail vehicles, the multiphysics modeling of mems, comprising vibrating micro-structures, and immersed in viscous fluids. He serves as a reviewer for several international journals.



ANTONIO LEANZA received the master's degree in mechanical engineering and the Ph.D. degree in engineering of complex systems from the University of Salento, in January 2017 and October 2021, respectively. He has a research experience with the University of Almería, Spain, regarding model-based estimation in multibody dynamics. He is currently a Researcher with the Politecnico di Bari. His research interests include vibration mechanics, mobile robotics, multibody dynamics, model-based estimation of mechanical systems, and automotive engineering.



SIMONE DE CAROLIS received the Ph.D. degree in mechanical engineering, in 2023. He is a Researcher with the Department of Mechanics, Politecnico di Bari. His research activities are related to the study of mechanical systems dynamics. His work focuses on system identification using input-output and output-only techniques, aimed at structural health monitoring and damage detection.



GIUSEPPE CARBONE received the M.Sc. degree in mechanical engineering and the Ph. D. degree in advanced production systems from the Politecnico di Bari, Italy, in February 1998 and February 2002, respectively. He is currently a Full Professor of applied mechanics and the Head of the Department of Mechanics Mathematics and Management, Politecnico di Bari; and the President of the Italian Tribology Association. In 2010, he has founded the Tribology Laboratory, Politecnico di Bari. He has

been a Visiting Scientist with the Juelich Research Center, Germany, and Eindhoven University of Technology, The Netherlands; an Academic Visitor with Imperial College London; and a Visiting Scholar with The University of North Texas. He is a Research Associate with the Institute of Photonics and Nanotechnologies, National Council of Research, Italy. He is a Founding Member of PoliMech s.r.l., a spin-off company of Politecnico di Bari. He has authored about 300 publications, of which about 165 in archive journals indexed in Scopus. His H-index is 40 (source: Scopus). His research has been funded from national and European programs and private companies with more than eight millions. His scientific interests focus mainly on tribology, contact mechanics, viscoelastic materials, adhesion, biomimetics, mechanical transmissions, mechanical vibrations, system dynamics, soft robotics grips, swarm intelligence, and complex systems. He serves as an Associate Editor of *Chaos, Solitons and Fractals* and *Frontiers in Mechanical Engineering* (Tribology Section). He is a member of the editorial board of *Tribology International*, *Biomimetics*, and *ISRN Tribology*. He also served as a Guest Editor for *Tribology International*, *Biomimetics*, *Coatings*, *Lubricants*, and *Applied Science*.

...